THE JOURNAL OF PHYSICAL CHEMISTRY C

Article

pubs.acs.org/JPCC

Thickness-Dependent Monoclinic Phases and Piezoelectric Properties Observed in Polycrystalline $(Pb_{0.94}La_{0.04})(Zr_{0.60}Ti_{0.40})O_3$ Thin Films

SiQi Zhang,[†,§] Fu Zheng,[†] ChenFei Jin,[†] and WeiDong Fei*[,‡]

[†]Department of Physics, Harbin Institute of Technology, Harbin 150001, People's Republic of China

[‡]Department of Physics and Chemistry, School of Materials Science and Engineering, Harbin Institute of Technology, Harbin 150001, People's Republic of China

Supporting Information

ABSTRACT: Ferroelectric thin films have received significant attention in view of their applications in microelectromechanical systems. Correlations between microstructure and polarization behavior have not been established. Polycrystalline $(Pb_{0.94}La_{0.04})(Zr_{0.60}Ti_{0.40})O_3$ thin films with thicknesses ranging from 100 to 400 nm were prepared on the $Pt(111)/Ti/SiO_2/Si(100)$ substrates by a sol–gel method. Synchrotron X-ray diffraction results revealed that the films thinner than 150 nm possess an asymmetry-allowed monoclinic (M_A) phase and undergo a M_A–monoclinic M_B–R phase sequence with increasing thickness. It was found that longitudinal piezoelectric coefficient d_{33} optimizes at 128 pm/V for 150 nm thick film. Above this thickness, a simple decreasing trend was observed. The presence of the monoclinic phase and (100) preferred orientation as well as crystalline quality are considered to play key roles in enhancing piezoelectric properties of the 150 nm thick film. Piezoelectric materials show a composition-related transition region where the crystal structure changes abruptly and the piezoelectric properties are maximal. In this study, an alternative approach is proposed in achieving excellent piezoelectric properties via a thickness-dependent constrain effect.

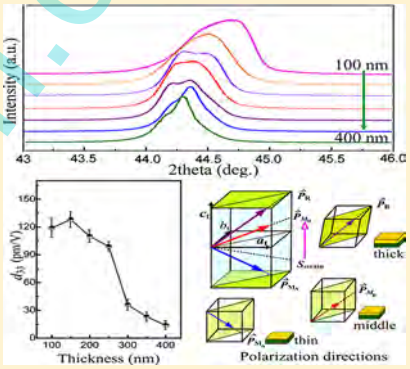

I. INTRODUCTION

Ferroelectric thin films including $PbTiO_3$(PT), $Pb(Zr_{1-x}Ti_x)O_3$ (PZT), La-doped PZT (PLZT), and $Pb(Mg_{1/3}Nb_{2/3}O_3)$-$x$$PbTiO_3$ (PMN-xPT) are of practical and academic interest because of their excellent piezoelectric, ferroelectric, electro-optic, and pyroelectric properties.[1−3] Excellent properties often tightly link with those coupling between polarization and thermodynamic "forces" such as temperature, stress, and electric field which makes them both interesting and very useful. Several researchers have explored the effects of these parameters on the phase diagram of epitaxial thin films, predicting new phases and piezoelectric properties and demonstrating changes in transition temperature.[4−6]Subsequently, for PZT-like perovskite ceramics, an intermediary monoclinic M_A phase between the tetragonal (T) and rhombohedral (R) phase near the morphotropic phase boundary (MPB, with a Zr/Ti ratio around 52/48) has been believed to be the origin of excellent piezoelectric properties of PZT bulk ceramics.[7−9] Further studies on bulk ceramics emphasize the significance of obtaining desired phase sequences under some conditions including the applied electric field direction and preferred orientation. There is a R–M_A–M_C–T phase sequence for applying electric field along the [001] direction in contrast with a field-induced R–M_b–O phase transformation for (110)-oriented PMN-30%PT ceramic.[10,11] It is also confirmed that the phase sequences in PMN-30%PT are distinctly different with the applied electric field along different crystallographic orientations including [001] and [110] directions.[12] Thus, it is important to establish correlations between microstructure and piezoelectric properties of ferroelectric thin films.

Generally, factors such as misfit strain/stress, grain size, and growth orientation are inevitable and significantly influence polarization and piezoelectric properties as dimensions continue to shrink.[13−15] It was found that niobium-doped PZT (PNZT) thin films exhibited a superior piezoelectric d_{33} coefficient of 307 pm/V near the so-called MPB (R–T phase boundary), and the MPB was shifted toward 70/30 instead of 52/48 due to the misfit compressive stress.[16] Further studies proposed that even for an identical 52/48 composition a thickness-dependent R–T phase transition can be induced in [100]-textured PNZT films where the d_{33} value reaches a maximum of 220 pm/V for an intermediate thickness around 350 nm.[17] Experimental studies confirmed that large remnant polarization changes can be induced by a thickness-independent mixture of (110) and (111) orientations for the $BiFeO_3$ thin films deposited on $SrRuO_3/Pt/TiO_2/SiO_2/Si(100)$ substrates.[18] Surely, studies on thickness-dependent piezoelectric properties as well as a R–T phase transition give

Received: July 7, 2015
Published: July 21, 2015

DOI: 10.1021/acs.jpcc.5b06517
J. Phys. Chem. C 2015, 119, 17487−17492

inspirations on optimizing piezoelectric properties of thin films. However, phase structures considering low-asymmetry monoclinic phases near the MPB of PZT-like films have not been carefully investigated. Actually, experimental studies aiming at condition-dependent phase sequences of ferroelectric thin films are made difficult by the limited sensitivity of various characterization techniques.

In the present study, by means of high-resolution synchrotron X-ray diffraction (XRD), thickness-dependent microstructure including phase structure, preferred orientation, and surface morphology and their possible influences on the piezoelectric properties of the $(Pb_{0.94}La_{0.04})(Zr_{0.60}Ti_{0.40})O_3$(PLZT) films are investigated. It is evidenced that the films can undergo a thickness-dependent $R-M_B-M_A$ phase sequence and possess as high as 128 pm/V piezoelectric coefficient d_{33} for the 150 nm thick film. The possible impact of phase sequence, preferred orientation type, and surface morphology on piezoelectric properties is discussed. The La/Zr/Ti composition of 4/60/40 is selected corresponding to the pure R phase in the composition phase diagram of PLZT/PZT bulk ceramics[19] based on our previous studies on PZT(55/45) and PZT(58/42) films[20] and PLZT (4/60/40) thick film.[21] It is demonstrated in this work that thickness-dependent new polarization rotation can occur in the films regardless of whether its Zr/Ti ratio is near the MPB composition. An alternative approach is proposed in achieving high quality thin films in terms of piezoelectric properties by means of thickness-dependent constrain effect.

II. EXPERIMENTAL METHODS

The sol–gel method was used in preparing thin films with thicknesses ranging from 100 to 400 nm on Pt(111)/Ti/SiO_2/Si(100) substrates, which has been described elsewhere.[22,23] 10% excess lead was added to the precursor solution to compensate for the loss of lead oxide during the annealing process. The composition of the precursor solution was designed as atomic ratios of La 0.04:Zr 0.60:Ti 0.40 which can ensure it lay in the pure phase region in the phase diagram of PLZT bulk ceramics. This composition is approximately consistent with the experimental analysis value of La 1.85:Zr 19.31:Ti 5.75 (wt %) measured by an atomic emission spectrometer (ICP-AES) suggesting an easy stoichiometry control for the sol–gel method. The thicknesses of the films were measured by a surface profile meter (Alpha-Step D-100, KLA-Tencor). Film crystalline structure was done by using a Philips X'pert XRD with Cu Kα radiation at 40 kV and 40 mA. For discriminating the possible phase coexistence, synchrotron XRD measurements were performed to characterize the overlapping profiles of $(110)_{pc}$, $(110)_{pc}$, and $(200)_{pc}$ diffractions at the beamline of 4B9A at the National Synchrotron Light Source (NSLS) with X-ray of about 15 keV from a Si(111) double-crystal monochromator. A Ge(111) double-crystal monochromator was used to provide an incident beam with a wavelength close to 0.54 Å giving an energy resolution of 3×10^{-4}. The surface morphology of the thin films and Raman spectra (532 nm in wavelength) were examined by using an atomic force microscope (AFM) integrated with confocal Raman microscopy (NT-MDT). The piezoelectric response of the thin films was observed by a commercial scanning force microscope (CSPM 5600 of Being Nano-Instruments, Ltd.) equipped with a lock-in amplifier (model SR530, Stanford Research Systems, Inc.). All scans were performed using a conductive Pt-coated monolithic silicon probe with an elastic constant of 40 N/m, a resonant frequency of 300 kHz, and an integrated tip of about 10 nm in diameter. The top platinum electrode with the same size of 3.14×10^{-4} cm^2 to the film under measurement was contacted with the conductive tip.

In our measurement, a sine voltage signal with an amplitude range between 0.5 and 3.5 V was input. By multiplying the deflection signal, the amplitude of the tip vibration was derived. The piezoelectric d_{33} coefficients were calculated from strain–voltage curves measured by applying the tip voltage pulses with variable amplitudes at a frequency of 5 kHz and by acquiring the piezoelectric response during each pulse. In the poling process, an electric field of 500 kV/cm was applied on a thin film for 10 min.

III. RESULTS AND DISCUSSION

Figure 1(a) shows the XRD $\theta-2\theta$ scan patterns of the films with thicknesses ranging from 100 to 400 nm. One can see that

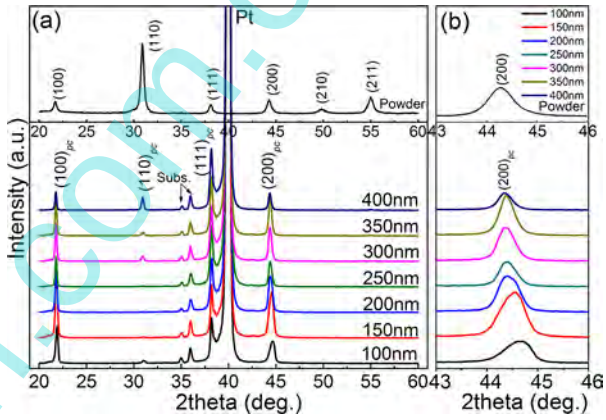

Figure 1. (a) XRD patterns of the films and (b) enlarged $(200)_{pc}$ diffraction. Inset shows typical XRD patterns of the stress-free PZT powder.

all the films crystallize in a single perovskite phase without an unwanted pyrochlore phase. Compared with the intensity of the (111) reflection, a higher intensity of (100)/(200) reflection suggests that the films thinner than 250 nm have a (100)-preferred orientation. However, it is found that the films thicker than 300 nm tend to have an increasing (111) reflection intensity as well as $(110)_{pc}$ reflection, suggesting an increasing dominant (111)-preferred orientation. In the past, the mechanisms of preferred orientations in PZT thin films have been investigated by some researchers.[24,25] Generally, ferroelectric PZT thin films have (111) preferred orientation on the Pt/Ti/SiO_2/Si substrates when nucleation and growth occur on the substrate surface. Possible reasons for the (100)-preferred orientation observed in the thinner films may be related to an enhanced self-textured growth in accordance with minimum surface energy conditions followed by La substitution. In contrast, (111)-oriented thick films could be attributed to those factors such as the lattice matching between substrate and the films, reducing interface effects, and an intermetallic phase $Pt_{5-7}Pb$. In Figure 1(b), $(200)_{pc}$ diffraction profiles for the thin films are asymmetric and with multiple peaks which differ from its R-structured bulk counterpart characterized by a singlet $(200)_{pc}$ diffraction peak (as shown in the inset). Also, the location of the $(200)_{pc}$ peak apparently shifts rightward in accordance with thickness alternation suggesting the thinner films are subject to large misfit strain as compared with those of

DOI: 10.1021/acs.jpcc.5b06517
J. Phys. Chem. C 2015, 119, 17487–17492

the thick films and the stress-free powder. For sol−gel-derived PZT thin films, large tensile stress generally builds up in the thinner films due to the lattice mismatch and different coefficients of thermal expansion between the film (6×10^{-6} K^{-1}) and the substrate (3.4×10^{-6} K^{-1}).[26]

Figure 2 illuminates the 3D surface morphology of all the films. A loose porous surface and defects such as cracks can be

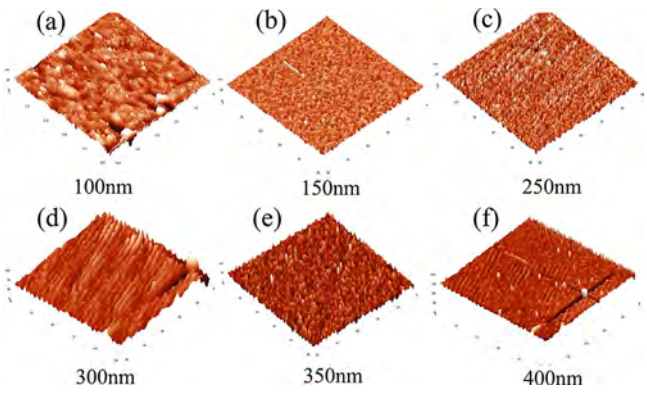

Figure 2. 3D surface morphology of the films with thicknesses ranging from 100 to 400 nm, in which the scan region includes (a) 5 μm × 5 μm and (b)−(f) 50 μm × 50 μm, respectively.

clearly observed in the 100 nm thick films as seen in Figure 2(a). As the thickness is slightly increased, the thin films thinner than 150 nm were grown into fine grains (~18 nm) and improved in surface uniformity in Figure 2(b),(c). A further increase in thickness leads the films with coarse grains (~35 nm) together with denser surfaces observed in Figure 2(d)−(f). Strikingly, the thicker films have regular and periodic stripelike surface structure with an approximate roughness S_A value of 3.2 nm. Possible reasons behind this stripe-like structure may connect to energetically favorable misfit-strain relaxation in the thicker films, followed by growing grain size once a film surpasses a critical thickness.[27]

For (100)-oriented polycrystalline thin films, the crystal phase can be characterized by three diffraction profiles including $(110)_{pc}$ at ψ = 45°, $(111)_{pc}$ at ψ = 54.7°, and $(200)_{pc}$ at ψ = 0° in a pseudocubic coordinate system. Figure 3 shows synchrotron XRD profiles on the $(110)_{pc}$ and $(111)_{pc}$ diffraction peaks of the films. As compared with those of the 400 nm film, either of the 100 nm film and 200 nm film exhibits broadening $(110)_{pc}$ and $(111)_{pc}$ diffraction profiles and has a location shifting toward low 2θ angles. For PLZT bulk ceramics, it is known that the *R* phase structure should exhibit double $(111)_{pc}$ peaks with an intensity ratio of 1:3 as well as singlet $(200)_{pc}$ diffraction. However, highly overlapping multiple peaks make it quite difficult to be used in determining possible phase structure of the films. Thus, asymmetric $(200)_{pc}$ diffraction profiles for the films at ψ = 0° were carefully examined.

Figure 4 shows asymmetry $(200)_{pc}$ diffraction peaks for the films at ψ = 0°. Several features can be described as follows. First, for the 100 nm and 150 nm thick films, an asymmetric $(200)_{pc}$ profile from Figure 4(a),(b) can be easily identified as double peaks with an intensity ratio of $(002)_{pc}/(200)_{pc}$ diffraction close to 1:2. Because the $(111)_{pc}$ and $(110)_{pc}$ diffraction profiles are not pure singlet, it excludes the possibility of the *T* phase and can be considered as M_A phase with *Cm* space group. Second, as the thickness is slightly

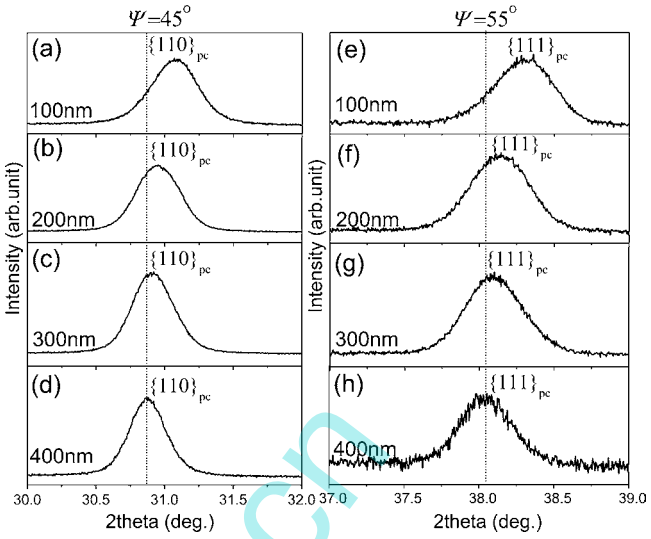

Figure 3. Synchrotron XRD experimental profiles on the $(110)_{pc}$ diffraction given by (a)−(d) and the $(111)_{pc}$ diffraction given by (e)−(h) for the films with thickness ranging from 100 to 400 nm.

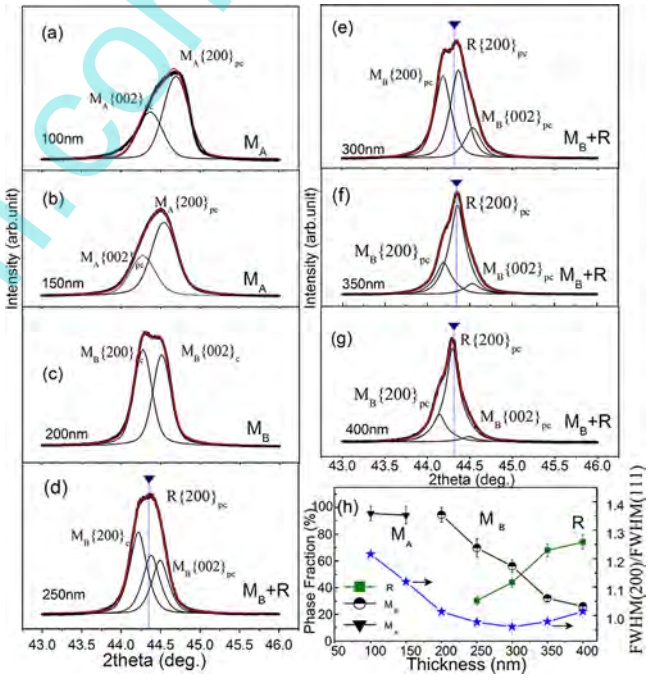

Figure 4. (a)−(g) Synchrotron XRD experimental profiles on the $(200)_{pc}$ diffraction of the films with thickness ranging from 100 to 400 nm, in which calculated profiles based on phase models and singlet $(200)_{pc}$ location for PLZT bulk ceramic with *R* phase are provided, and (h) thickness-dependent ratio of fwhm (200)/fwhm $(111)_{pc}$ and calculated phase fraction of the films corresponding to M_A, M_B, and *R*, respectively.

increased beyond 200 nm, the diffraction shape shown in Figure 4(c) changes abruptly with an obvious intensity ratio of $(002)_{pc}/(200)_{pc}$ diffraction close to 1:1 which suggests a phase transition from M_A to another phase. An intermediate M_B phase with an identical *Cm* space group is assumed if results are referenced to that of Singh et al.[28] Third, for the films thicker than 250 nm shown in Figure 4(d)−(g), $(200)_{pc}$ diffraction profiles change again, and a third shoulder is observed with much lower intensity than those of the others. Typically,

DOI: 10.1021/acs.jpcc.5b06517
J. Phys. Chem. C 2015, 119, 17487−17492

$(200)_{pc}$ diffraction profiles for the 300 nm film can be distinguished as three peaks. Because the films have a similar 2θ angle (~44.3°) with its bulk counterpart, the "*R*-like" phase (*R*3*c* space group) coexisting with the M_B phase is reasonably considered, assuming that an infinite thick film exhibits reducing misfit strain/stress and similar phase component to its bulk ceramics.[29] For the 350 nm and 400 nm thick films, the (200) diffraction peak shapes in Figure 4f,g are stable and similar to that of the 300 nm thick film suggesting an identical coexistence of *R* and M_B phases.

By using a Psdvoigt2 peak-fitting function, (200) profiles of the films are calculated based on proposed phase models. As seen in Figure 4(a)−(g), the fit errors between the experimental and the calculated profiles are quite small, which support proposed phase models. Figure 4(h) gives the phase fraction and fwhm $(200)_{pc}$/fwhm $(111)_{pc}$ ratio dependence on thickness of the films. It is seen that the films above 200 nm have an increasing *R* phase fraction from 30% to 80%. Additionally, with the increasing thickness, the ratios of fwhm $(200)_{pc}$/fwhm $(111)_{pc}$ also change, suggesting different phase structures. Thus, the critical thicknesses for the films corresponding to M_A−M_B (dominant) and M_B−*R* (dominant) phase transitions are 200 and 300 nm, respectively.

To see clearly the appearance of a small third shoulder at room temperature, Figure 5 provides typical temperature-dependent synchrotron XRD $(200)_{pc}$ profiles for the 300 nm thick film. As temperature is raised above 200 °C, the third peak can be seen and has a 2θ shifting trend toward low angles in accordance with temperature-related strain/stress modification. Besides, there is no abrupt change on the shape of $(200)_{pc}$ diffraction suggesting identical phase components.

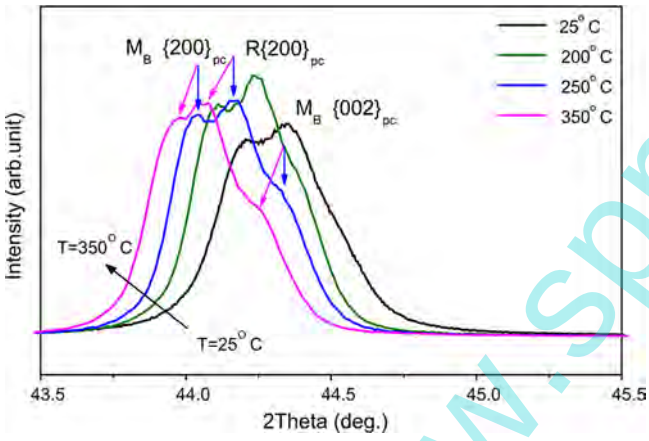

Figure 5. Temperature-dependent synchrotron XRD profiles for the 300 nm thick film.

Figure 6 shows the Raman spectrum of the PLZT samples at room temperature with the modes identified according to the Raman spectra of $PbTiO_3$ (PT) tetragonal material.[30] From Figure 6(a), it is obviously observed that all the films and stress-free PLZT powder display wide Raman spectra as compared with sharp and well-defined Raman bands of PT tetragonal single crystal. For the thick films with thickness higher than 300 nm, more broad Raman bands including E(2TO), E + B1, and A_1(2TO) in the range of 100−400 cm^{-1} cause an obvious overlapping in Raman soft modes as observed in PLZT(4/65/35) bulk ceramics.[31,32] Marssi et al.[33] predict that oxygen octahedral tilt disorder together with more complex domain

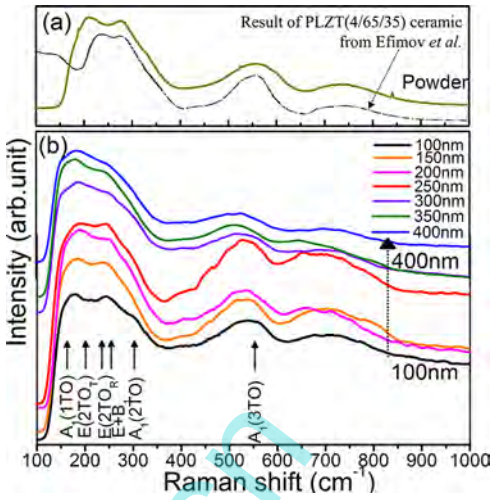

Figure 6. (a) Raman spectra of the PLZT powder including the results obtained in the present work and results from Eflmov et al.[32] and (b) of the films with different thicknesses ranging from 100 to 400 nm.

geometries (71°/109°) presenting for rhombohedral-structured PLZT ceramics prevent any partial Raman selection rules (RSR) from occurring. Also effects including high internal stresses, polarization nonuniformity, and size-related effects play roles in broadening the Raman bands.[34,35] Typically, for the 400 nm thick film, the A_1 (TO_2) peak related to the displacement of Ti and O atoms relative to Pb atoms along the opposite direction disappears and evolves into a broad *R*-structured transverse mode. Moreover, the A_1(3TO) mode also has a shifting trend toward low wave numbers with an increasing thickness, which might be in accordance with a relaxed misfit strain between the film and the substrate.[36] In contrast, this mode of the *R*-structured PLZT(4/60/40) and PLZT(6/65/35) powder locates at high wavenumber around 550 cm^{-1}. Thus, in light of studies on PLZT ceramics, these changes on Raman bands can be taken as a signal of *R* phase existing in the films with thickness above 300 nm. Additionally, the *R*-structured powder exhibits poor similarity on the Raman spectrum with those of the thick films. We suspect that more complicated contributions for the Raman spectrum than XRD analysis might play roles, although possible mechanisms are still lacking. However, the A_1 (TO_2) peak (~330 cm^{-1}) for the thin films becomes sharper with higher Raman intensity than that of the thick films. According to Filho et al.,[37] this increase is related to changes in the polarization implying the existence of a tetragonal phase for the PZT system. Especially, the 100 nm thick film has similar Raman profiles with that of monoclinic-structured $Pb(Zr_{0.53}Ti_{0.47})O_3$ bulk ceramics. So, this observation also predicts the presence of monoclinic *Cm* symmetry in the thin films (typically for the 100 nm thick film).

Figure 7 gives the thickness-dependent d_{33} values and possible strain-driven polarization rotation of the films. It can be seen that in thin films prepared there is a decreasing piezoelectric coefficient d_{33} tendency in which an optimal value obtained for the 150 nm film is around 128 pm/V. Although d_{33} values observed in PLZT thin films are not ideal as compared with those of the PNZT films,[16,17] they remain higher than those of 60 pm/V reported in PZT thin films with 52/48 composition.[38−40] If compared with the 100 nm film, the d_{33} value slowly decreases to 17% for the thickness below 250 nm and decreases to 88% for the thickness below 400 nm. Besides, as compared with that of the 150 nm thick film, a slight

DOI: 10.1021/acs.jpcc.5b06517
J. Phys. Chem. C 2015, 119, 17487−17492

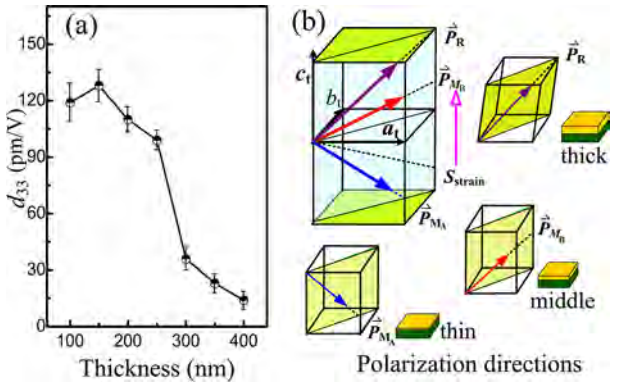

Figure 7. (a) Thickness-dependent piezoelectric coefficients in the films and (b) scheme of the polarization directions of the films.

decreasing d_{33} value for the 100 nm thick film can be attributed to its poor quality and inferior (100)-preferred orientation due to its porous surface, defect, and intermediate layer.[41]

Higher piezoelectric coefficients of the (100)-oriented thin films can be explained by the polarization rotation mechanism.[42] Figure 7(b) illustrated several polarization directions of the films. For the thicker films with (111)-preferred orientation, because its (111) surface lies parallel to the surface plane and polarization component of *R* phase component is fixed along $\langle 111 \rangle_{pc}$ directions, it is rather difficult to adjust itself to applied electric field along the *z*-axis direction, resulting in poor piezoelectric d_{33} values. In contrast, for the (100)-preferred thin films, although the spontaneous polarization of the thinner films with larger misfit strain/stress may not change absolute magnitude, it can be rotated out-of-plane through the monoclinic (M_A or M_B) symmetry plane. Specially, in terms of monoclinic phase, although monoclinic M_A and M_B phases belong to the same space group *Cm* and similar unit cells, their magnitudes of polarization components (*P*) are different: for the M_A phase, $P_x = P_y < P_z$, but for the M_B phase, $P_x = P_y > P_z$. Thus, for the (100)-oriented films under large misfit strain, more in-plane polarization increments can be expected for the M_A phase along the *c*-axis direction than the M_B phase as well as *R* phase under an applied electric field. These observations lend further support to the results by synchrotron XRD in $PbTiO_3$ thin films under tensile strain which possess stripe domains and a polarization rotation away from the tetragonal axis.[43]

IV. CONCLUSIONS

PLZT (4/60/40) thin films with thicknesses ranging from 100 to 400 nm deposited on Pt(111)/Ti/SiO_2/Si(100) substrates were prepared by using sol−gel methodology. For films thicker than 300 nm, regular periodic stripe-like surface structures are observed partly due to internal stress alternation of the thick films followed by grain size increase. Synchrotron XRD data suggested the presence of a thickness-dependent R−M_B−M_A phase sequence, and the fraction of monoclinic phases decreases with increasing thickness. Piezoelectric measurements suggest that the 150 nm thick film exhibits an optimal piezoelectric coefficient of 128 pm/V. The presence of low symmetry monoclinic M_A phase and (100) preferred orientation as well as crystalline quality are considered to be crucial in enhancing piezoelectric properties of the thin films. Our studies present an alternative approach for achieving good piezoelectric thin films just by means of thickness-dependent constrain effect. This could have important practical implications since these phases are known to be responsible for piezoelectric responses in complex systems.

■ ASSOCIATED CONTENT

Supporting Information

The Supporting Information is available free of charge on the ACS Publications website at DOI: 10.1021/acs.jpcc.5b06517.

Table S1. Parameters on calculating the piezoelectric coefficients of the films. Figure S1. Linear-fitted experimental data for obtaining longitudinal d_{33} values of the films (PDF)

■ AUTHOR INFORMATION

Corresponding Author

*Fax/Tel.: +86-451-86413908. E-mail: wdfei@hit.edu.cn.

Present Address

[§]Key Laboratory of Micro-Optics and Photonic Technology of Heilongjiang Province.

Notes

The authors declare no competing financial interest.

■ ACKNOWLEDGMENTS

We would like to gratefully acknowledge the support of National Synchrotron Light Source in Institute of High Energy Physics, Chinese Academy of Sciences, in providing the synchrotron XRD facilities used in this work. One of the authors (S.Q. Zhang) wants to express her gratitude to Micro-Optics and Photonic Technology Laboratory, Harbin Institute of Technology, China, in providing Raman spectra measurement. This work is supported by the Fundamental Research Funds for the Central Universities and Program for Innovation Research of Science in Harbin Institute of Technology (PIRS of HIT, No. B201503) and the Fundamental Research Funds for the Central Universities(Grant HIT NSRIF. 2011012), as well as The National Natural Science Foundation of China (Grant 61102147 and U1432104).

■ REFERENCES

(1) Damjanovic, D. Ferroelectric, Dielectric and Piezoelectric Properties of Ferroelectric Thin Films and Ceramics. *Rep. Prog. Phys.* **1998**, *61*, 1267.

(2) Yourdkhani, A.; Caruntu, G. Characterization of the Microstructural and Piezoelectric Propertiesof $PbTiO_3$Thin Films Synthesized by Liquid-Phase Deposition. *J. Phys. Chem. C* **2011**, *115*, 14797−14805.

(3) Park, H. H.; Kim, W. S.; Yang, J. K.; Park, H.-H.; Hill, R. H. Characterization of PLZT Thin Film Prepared by Photo-Chemical Deposition Using Photosensitive Metal-Organic Precursors. *Microelectron. Eng.* **2004**, *71*, 215−220.

(4) Pertsev, N. A.; Zembilgotov, A. G.; Tagantsev, A. K. Effect of Mechanical Boundary Conditions on Phase Diagrams of Epitaxial Ferroelectric Thin Films. *Phys. Rev. Lett.* **1998**, *80*, 1988.

(5) Qiu, J. H.; Jiang, Q. Effects of External Mechanical Loading on Phase Diagrams and Dielectric Properties in Epitaxial Ferroelectric Thin Films with An-isotropic In-plane Misfit Strains. *J. Appl. Phys.* **2007**, *101*, 034110.

(6) Li, Y. L.; Choudhury, S.; Liu, Z. K.; Chen, L. Q. Effect of External Mechanical Constraints on the Phase Diagram of Epitaxial $PbZr_{1-x}Ti_xO_3$Thin Films-Thermodynamic Calculations and Phase-Field Simulations. *Appl. Phys. Lett.* **2003**, *83*, 1608−1610.

(7) Noheda, B.; Cox, D. E.; Shirane, G.; Gonzalo, J. A.; Cross, L. E.; Park, S. E. A Monoclinic Ferroelectric Phase in the $Pb(Zr_{1-x}Ti_x)O_3$ Solid Solution. *Appl. Phys. Lett.* **1999**, *74*, 2059−2061.

(8) Guo, R.; Cross, L. E.; Park, S.-E.; Noheda, B.; Cox, D. E.; Shirane, G. Origin of the High Piezoelectric Response in $Pb(Zr_{1-x}Ti_x)O_3$. *Phys. Rev. Lett.* **2000**, *84*, 5423−5426.
(9) Noheda, B.; Gonzalo, J. A.; Cross, L. E.; Guo, R.; Park, S. E.; Cox, D. E.; Shirane, G. Tetragonal-to-Monoclinic Phase Transition in a Ferroelectric Perovskite: The Structure of $PbZr_{0.52}Ti_{0.48}O_3$. *Phys. Rev. B: Condens. Matter Mater. Phys.* **2000**, *61*, 8687−8695.
(10) Bai, F. M.; Wang, N. G.; Li, J. F.; Viehland, D.; Gehring, P. M.; Xu, G. Y.; Shirane, G. X-Ray and Neutron Diffraction Investigations of the Structural Phase Transformation Sequence Under Electric field in $0.7Pb(Mg_{1/3}Nb_{2/3})$-$0.3PbTiO_3$Crystal. *J. Appl. Phys.* **2004**, *96*, 1620−1627.
(11) Viehland, D.; Li, J. F. An hysteretic Field-induced Rhombohedral to Orthorhombic Transformation in (110)-Oriented 0.7Pb $(Mg_{1/3}Nb_{2/3})O_3$-$0.3PbTiO_3$ Crystals. *J. Appl. Phys.* **2002**, *92*, 7690−7692.
(12) Cao, H.; Bai, F. M.; Wang, N. G.; Li, J. F.; Viehland, D.; Xu, G. Y.; Shirane, G. Intermediate Ferroelectric Orthorhombic and Monoclinic M_B Phases in [110] Electric-Field-Cooled Pb-$(Mg_{1/3}Nb_{2/3})O_3$-30%$PbTiO_3$ Crystals. *Phys. Rev. B: Condens. Matter Mater. Phys.* **2005**, *72*, 064104.
(13) Lian, L.; Sottos, N. R. Effects of Thickness on the Piezoelectric and Dielectric Properties of Lead Zirconate Titanate Thin Films. *J. Appl. Phys.* **2000**, *87*, 3941.
(14) Ren, S. B.; Lu, C. J.; Liu, J. S.; Shen, H. M.; Wang, Y. N. Size-Related Ferroelectric-Domain- Structure Transition in a Polycrystalline PbTiO3 Thin Film. *Phys. Rev. B: Condens. Matter Mater. Phys.* **1996**, *54*, 14337.
(15) Ambika, D.; Kumar, V.; Imai, H.; Kanno, I. Sol-gel Deposition and Piezoelectric Properties of {110}-Oriented $Pb(Zr_{0.52}Ti_{0.48})O_3$Thin Films. *Appl. Phys. Lett.* **2010**, *96*, 031909.
(16) Zhu, Z. X.; Li, J. F.; Liu, Y. Y.; Li, J. Y. Shifting of the Morphotropic Phase Boundary and Superior Piezoelectric Response in Nb-doped $Pb(Zr,Ti)O_3$Epitaxial Thin Films. *Acta Mater.* **2009**, *57*, 4288−4295.
(17) Li, J. F.; Zhu, Z. X.; Lai, F. P. Thickness-Dependent Phase Transition and Piezoelectric Response in Textured Nb-Doped $Pb(Zr_{0.52}Ti_{0.48})O_3$ Thin Films. *J. Phys. Chem. C* **2010**, *114*, 17796−17801.
(18) Wu, J. G.; Wang, J.; Xiao, D. Q.; Zhu, J. G. Ferroelectric Behavior in Bismuth Ferrite Thin Films of Different Thickness. *ACS Appl. Mater. Interfaces* **2011**, *3*, 3261−3263.
(19) Haertling, G. H. Ferroelectric Ceramics: History and Technology. *J. Am. Ceram. Soc.* **1999**, *82*, 797−818.
(20) Wang, J. N.; Li, W. L.; Li, X. L.; Fei, W. D. Rhombohedral-Monoclinic Phase Transition Related to Grain Orientation in Zr-rich $Pb(Zr_xTi_{1-x})O_3$Thin Films. *J. Alloys Compd.* **2011**, *509*, 3398−3402.
(21) Zhang, S. Q.; Wang, L. D.; Li, W. L.; Li, N.; Fei, W. D. Effects of Lanthanum Doping on the Preferred Orientation, Phase Structure and Electrical Properties of Sol−gel Derived $Pb_{1-3x/2}La_x(Zr_{0.6}Ti_{0.4})O_3$Thin Films. *J. Alloys Compd.* **2011**, *509*, 2976−2980.
(22) Tahan, D. M.; Safari, A.; Klein, L. C. Preparation and Characterization of $Ba_xSr_{1-x}TiO_3$Thin Films by a Sol-gel Technique. *J. Am. Ceram. Soc.* **1996**, *79*, 1593−1598.
(23) Zhang, S. Q.; Fei, W. D.; Li, W. L.; Wang, J. N. Ferroelectric Properties of Highly (111)-Oriented $Pb(Zr_{1-x}, Ti_x)O_3$Thin Films with Different Zr/Ti Ratios. *J. Alloys Compd.* **2009**, *487*, 703−707.
(24) Chen, S. Y. Texture Evolution and Electrical Properties of Oriented PZT Thin Films. *Mater. Chem. Phys.* **1996**, *45*, 159−162.
(25) Chen, S. Y.; Chen, I. W. Texture Development, Microstructure Evolution, and Crystallization of Chemically Derived PZT Thin Films. *J. Am. Ceram. Soc.* **1998**, *81*, 97−105.
(26) Brennecka, G. L.; Huebner, W.; Tuttle, B. A.; Clem, P. G. Use of Stress to Produce Highly Oriented Tetragonal Lead Zirconate Titanate (PZT 40/60) Thin Films and Resulting Electrical Properties. *J. Am. Ceram. Soc.* **2004**, *87*, 1459−1465.
(27) Matthews, J. W.; Blakeslee, A. E. Defects in Epitaxial Multilayer: I. Misfit Dislocations. *J. Cryst. Growth* **1974**, *27*, 118−125.
(28) Singh, A. K.; Pandey, D. Confirmation of M_B-Type Monoclinic Phase in $Pb[(Mg_{1/3}Nb_{2/3})_{0.71}Ti_{0.29}]O_3$: A powder Neutron Diffraction Study. *Phys. Rev. B: Condens. Matter Mater. Phys.* **2003**, *68*, 172103.
(29) Zhang, S. Q.; Wang, L. D.; Li, W. L.; Liu, C. Q.; Wang, J. N.; Li, N.; Darvishi, A. R.; Fei, W. D. Stress-Induced Shifting of the Morphotropic Phase Boundary in Sol-gel Derived $Pb(Zr_{0.5}Ti_{0.5})O_3$ Thin Films. *Mater. Res. Bull.* **2011**, *46*, 1237−1242.
(30) Frantti, J.; Lantto, V. Structural Studies of Nd-modified Lead Zirconate Titanate Ceramics Between 11 and 680 K at the Morphotropic Phase Boundary. *Phys. Rev. B: Condens. Matter Mater. Phys.* **1997**, *56*, 221−236.
(31) Zhang, Y.; Cheng, X.; Zhang, S. In-situ Raman Spectroscopic Study of Domain Switching of PLZT Ceramics. *Appl. Phys. A: Mater. Sci. Process.* **2007**, *89*, 685−693.
(32) Efimov, V. V.; Efimova, E. A.; Iakoubovskii, K.; Khasanov, S.; Kochubey, D. I.; Kriventsov, V. V.; Kuzmin, A.; Mavrin, B. N.; Sakharov, M.; Sikolenko, V.; et al. EXAFS, X-Ray Diffraction and Raman Studies $(Pb_{1-x}La_x)$ $(Zr_{0.65}Ti_{0.35})O_3$ (x = 0.04 and 0.09) Ceramics Irradiated by High-Current Pulsed Electron Beam. *J. Phys. Chem. Solids* **2006**, *67*, 2007−2012.
(33) Marssi, M. E.; Farhi, R.; Picot, J. C.; Viehland, D. Raman Selection Rules and Relaxor Ferroelectric Behavior in PLZT Compounds. *Ferroelectrics* **1997**, *201*, 101−106.
(34) Prater, R. L.; Chase, L. L.; Boatner, L. A. Raman Scattering Studies of the Impurity-Induced Ferroelectric Phase Transition in $KTaO_3$:Li. *Phys. Rev. B: Condens. Matter Mater. Phys.* **1981**, *23*, 5904.
(35) Bykov, I. P.; Glinchuk, M. D.; Laguta, V. V.; Maximenko, Y. L.; Jastrabik, L.; Trepakov, V. A.; Dimza, V.; Hrabovsky, M. Investigation of Chromium Impurities Charge State and Chemical Bonds in PLZT Ceramic. *J. Phys. Chem. Solids* **1995**, *56*, 919−923.
(36) Xu, W.-H.; Lu, D.; Zhang, T.-Y. Determination of Residual Stresses in $Pb(Zr_{0.53}Ti_{0.47})O_3$ Thin Films with Raman Spectroscopy. *Appl. Phys. Lett.* **2001**, *79*, 4112−4114.
(37) Filho, A. G. S.; Lima, K. C. V.; Ayala, A. P.; Guedes, I.; Freire, P. T. C.; Melo, F. E. A.; Filho, J. M.; Araújo, E. B.; Eiras, J. A. Raman Scattering Study of the $PbZr_{1-x}Ti_xO_3$ System: Rhombohedral-Monoclinic-Tetragonal Phase Transitions. *Phys. Rev. B: Condens. Matter Mater. Phys.* **2002**, *66*, 132107.
(38) Zavala, G.; Fendler, J. H.; Trolier-McKinstry, S. Characterization of Ferroelectric Lead Zirconate Titanate Films by Scanning Force Microscopy. *J. Appl. Phys.* **1997**, *81*, 7480.
(39) Haccart, T.; Cattan, E.; Remiens, D.; Hiboux, S.; Muralt, P. Evaluation of Niobium Effects on the Longitudinal Piezoelectric Coefficients of $Pb(Zr,Ti)O_3$Thin Films. *Appl. Phys. Lett.* **2000**, *76*, 3292−3294.
(40) Berfield, T. A.; Ong, R. J.; Payne, D. A.; Sottos, N. R. Residual Stress Effects on Piezoelectric Response of Sol-gel Derived Lead Zirconate Titanate Thin Films. *J. Appl. Phys.* **2007**, *101*, 024102.
(41) Habouti, S.; Lahmar, A.; Dietze, M.; Solterbeck, C. H.; Zaporojtchenko, V.; Es-Souni, M. Substrate Hetero-structure Effects on Interface Composition, Microstructure Development and Functional Properties of PZT Thin Films. *Acta Mater.* **2009**, *57*, 2328−2338.
(42) Fu, H.; Cohen, R. E. Polarization Rotation Mechanism for Ultrahigh Electromechanical Response in Single-Crystal Piezoelectrics. *Nature* **2000**, *403*, 281−283.
(43) Catalan, G.; Janssens, A.; Rispens, G.; Csiszar, S.; Seeck, O.; Rijnders, G.; Blank, D. H. A.; Noheda, B. Polar Domains in Lead Titanate Films Under Tensile Strain. *Phys. Rev. Lett.* **2006**, *96*, 127602.

DOI: 10.1021/acs.jpcc.5b06517
J. Phys. Chem. C 2015, 119, 17487−17492